

DEFECT EVOLUTION AND STRUCTURAL IMPROVEMENT IN LOW ENERGY ION IRRADIATED CARBON NANOTUBES: MICROSCOPIC AND SPECTROSCOPIC STUDIES

DILIP K. SINGH

*Centre for Nanotechnology, Indian Institute of Technology Guwahati
Guwahati, Assam-781039, India
s.dilip@iitg.ernet.in*

PARAMESHWAR K. IYER

*Department of Chemistry, Indian Institute of Technology Guwahati
Guwahati, Assam-781039, India*

P. K. GIRI

*Department of Physics, Indian Institute of Technology Guwahati
Guwahati, Assam-781039, India*

The capability of graphitic networks to reorganize their structures under irradiation of energetic particles provides the tool for nano-engineering of carbon nanotubes (CNTs). We have studied the effect of 30 keV N^+ ion irradiation with three different fluences 10^{12} , 10^{13} , and 10^{14} ions/cm² on the structural and spectroscopic properties of single-walled carbon nanotubes (SWNTs) and multiwalled carbon nanotubes (MWNTs). Irradiation-induced structural defects and coalescence of the nanotubes are studied using high-resolution transmission electron microscopy (HRTEM). Upon irradiation, some of the radial breathing modes in Raman spectra disappear due to conversion from single-walled to multiwalled structure. We observed a systematic change in intensity of the intermediate frequency mode (IFM) with increasing dose of ion-irradiation and these IFM modes are attributed to structural defects of SWNTs. Dramatic improvement in the intensity ratio G-band to D-band (at ~ 1335 cm⁻¹) for ion fluence of 10^{13} ions/cm² indicates improved graphitic structure as a result of reconstruction. Similarly, X-ray Photoelectron spectroscopy studies show improvement in the amount of sp^2 carbon upon 10^{13} ions/cm² N^+ ion irradiation dose. At a higher dose (10^{14} N^+ ions/cm²), vacancy and bent structures having Stone–Wales defects were observed in HRTEM, whereas MWNTs show formation of surface hillock like protrusions leading to formation of fullerene-like structures.

Keywords: Carbon nanotubes; defects; ion-irradiation; HRTEM; Raman; XPS.

1. Introduction

Structural defects in the carbon nanotubes (CNTs) have been found to play a critical role in improving the characteristic properties required for future potential applications. Structural defects like vacancies have been found to improve the gas-sensing properties

greatly.¹ Defective CNTs have been observed to show higher photoconductivity due to the creation of new electronic states favorable for large area light sensor and nano-optoelectronic devices.² A number of literature focused on spectroscopic properties of structural defects in CNTs.^{3,4} Modification of Raman

spectral modes upon irradiation has been a subject of discussion in literature.⁵ But very few of them establish the origin of intermediate frequency modes (IFM) in the Raman spectra.

The irradiation-induced structural transformation in CNTs are due to defects mainly in the form of vacancies and interstitials and the dominant mechanism for defect creation is the knock on atomic displacements due to kinetic energy transfer.⁶ Trapping of electrons by vacancies can create extrinsic holes in the π -band. Various ranges of energies, fluences, and nature of ions modify the CNT structure in different ways. Krashennikov *et al.* have introduced the effect of ion-irradiation on CNTs and possibility of engineering nanostructured carbon materials with electron or ion beams.^{6,7} The possibility of controlled modification of electronic and optical properties of CNTs through ion irradiation has been explored in this work.

2. Experimental Details

For the present study CNTs grown by catalytic chemical vapor deposition using metal catalysts and subsequent acid purification were used and these are procured from Shenzhen Nanotech, China. SWNTs of diameter less than 2 nm and length 5–15 μm , and MWNTs of diameter range 10–20 nm and length 5–15 μm were used for irradiation. Samples for irradiation were prepared using multiple drop casting the well-dispersed solution of CNTs in ethanol on silicon wafer of size 2 cm \times 2 cm of thickness 10 μm approximately. Samples were implanted at 30 KeV with nitrogen ($^{14}\text{N}^+$) ion-beam to fluence levels 10^{12} , 10^{13} , and 10^{14} ions/cm². These samples are referred as SWNT0 (before irradiation), SWNT12 (after 10^{12} ions/cm² N^+ dose), SWNT13 (after 10^{13} ions/cm² N^+ dose), and SWNT14 (after 10^{14} ions/cm² N^+ dose) for SWNTs. Similarly, MWCNT after 10^{13} N^+ ions/cm² dose is referred as MWCNT13. Samples were implanted at normal incidence using a 150 KeV ion accelerator. During implantation a vacuum of 1.0×10^{-6} mbar was maintained in the target chamber. A portion of the samples was scratched out from silicon wafer and were used for other spectroscopic measurements. Morphological characterization was done using High-resolution (HR) JEOL 2010 TEM. Raman spectra were recorded in backscattering mode using 488 nm Ar^+ ion laser. XPS studies were performed on a VG instrument with a Mg K_α source at an emission angle of 30°.

3. Results and Discussion

3.1. HRTEM studies

HRTEM images of SWNTs before irradiation shown in Fig. 1(a) show perfect tubular structure. Irradiation dose of 10^{12} ions/cm² of N^+ irradiation leads to the formation of small number of carbon vacancies in the structure but majority of the tubes remains intact as shown in Fig. 1(b). HRTEM images of SWNTs after a dose 10^{13} N^+ ions/cm² show sectioning of SWNTs (marked as α) along with the presence of amorphous carbon (marked as β) as shown in Fig. 1(c). MWNTs present in the SWNTs samples as impurities are comparatively more damaged as clearly evident from TEM images and amorphous carbon deposits are preferably from MWNTs. Figure 1(d) show heavy damage of tubular structure of carbon after 10^{14} N^+ ions/cm² irradiation dose. Figure 1(e) shows amorphous carbon deposits (marked as γ), surface vacancies (marked as δ) and Fig. 1(f) show HRTEM image of number of vacancies (indicated as σ , ρ , and τ) after dose of 10^{14} ions/cm². Figure 1(g) shows that higher dose of 10^{14} ions/cm² leads to renucleation of amorphous carbon resulting in nanospring like structure of carbon observed at few places. HRTEM images further reveal that these are made up of small linear chains of carbons of length ~ 20 nm and double-layered fullerene structures at the ends arranged in the order to form nanospring-like structural features. Ion-irradiation leads to the formation of curved carbon nanostructures in case of MWNTs (indicated as ϕ) in contrast to SWNTs shown in Fig. 1(h), which takes shape of fullerenes with increasing dose.

3.2. Raman analysis

Low-frequency radial breathing modes (RBM) characteristic of SWNTs diameter, gradually disappear with increasing irradiation dose as shown in Fig. 2(a). It is possible with complete destruction of tubular nature of the CNTs which is not the case as observed in HRTEM. In fact, structural transformation of SWNTs bundles into MWNTs leading to modification in RBM intensity. Figure 2(b) show that defect-related new feature evolves in the IFMs (observed in the range 400–1200 cm^{-1}) as a result of ion irradiation. Raman active peak at 668.9 cm^{-1} observed in case of virgin MWNTs disappears, and new features at 926 and 1033 cm^{-1} appear upon 10^{12} ions/cm² irradiation dose. Besides these peaks,

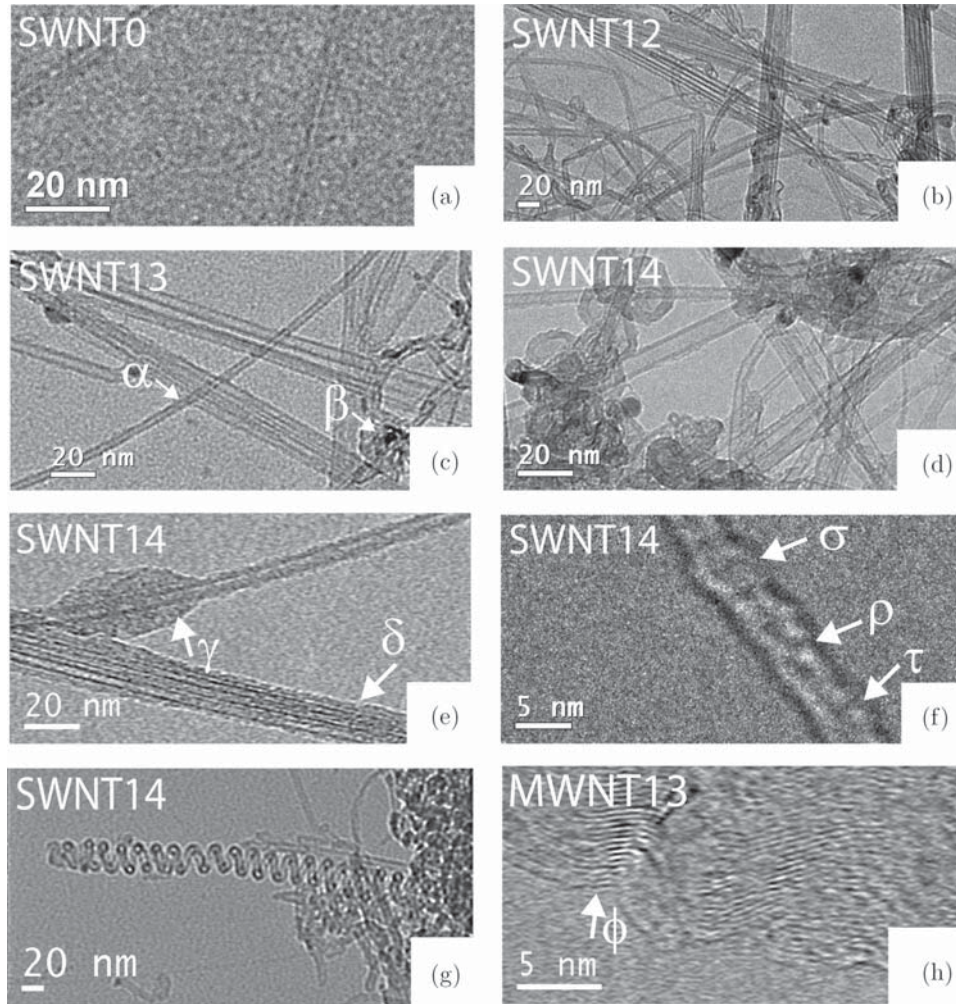


Fig. 1. TEM image of SWNTs and MWNTs before and after irradiation. Arrows with α show sectioning of nanotubes, β shows amorphous carbon formed, γ and δ show the large number of surface vacancies formed after a dose of 10^{14} N^+ ions/cm². High-resolution image of the surface vacancies are shown by σ , ρ , and τ . Region ϕ shows the formation of curved graphitic structure in case of MWNTs.

two small hump-like features at ~ 805 and 868 cm^{-1} were observed which are significantly enhanced upon 10^{14} ions/cm² irradiation dose. Lorentzian fits to these IFM modes show their positions at 804.9, 867.8, 926, and 935.3 cm^{-1} (shown in inset of Fig. 2(b)). Among these, 926 cm^{-1} feature is the most intense and sharpest peak having FWHM of 14.2 cm^{-1} . Along with these a clear peak is observed at 935.3 cm^{-1} having almost similar FWHM (14.6 cm^{-1}). Other two features observed at 804.9 and 867.8 cm^{-1} have FWHM 33.1 and 25.5 cm^{-1} , respectively. The origin of these features is not clearly understood in literature. According to group theory, it should be a Raman-silent region for infinitely long tube.⁸ Some studies conclude that IFM modes are related to the finite size defects of carbon nanotubes.⁹ These new Raman modes observed upon irradiation were assigned to the phonon density of states arising due to structural defects and overtones

of the defect-induced peaks. Using 30 keV Ar^+ ion irradiation, Roth *et al.* have shown that IFM modes originate as a result of modification of phonon density of states due to creation of defects.¹⁰ Our experiment clearly demonstrates that 804, 868, and 926 cm^{-1} Raman modes are primarily due to the local structural defects introduced upon ion irradiation. On the other hand, 668.9 cm^{-1} mode is characteristic of the nanotubes, as the intensity of this peak improves with the structural improvement.

Figure 3(a) show the characteristic Raman modes known as D-band and G-band. Inset shows the deconvolution of these spectra for lineshape analysis. Except the line indicated as Fano, all other components are Lorentzian in shape. Irradiated CNTs show a peak at 1402 cm^{-1} due to distortion of the graphene network upon ion-irradiation. A dose of 10^{13} ions/cm² leads to increase of intensity of G-band

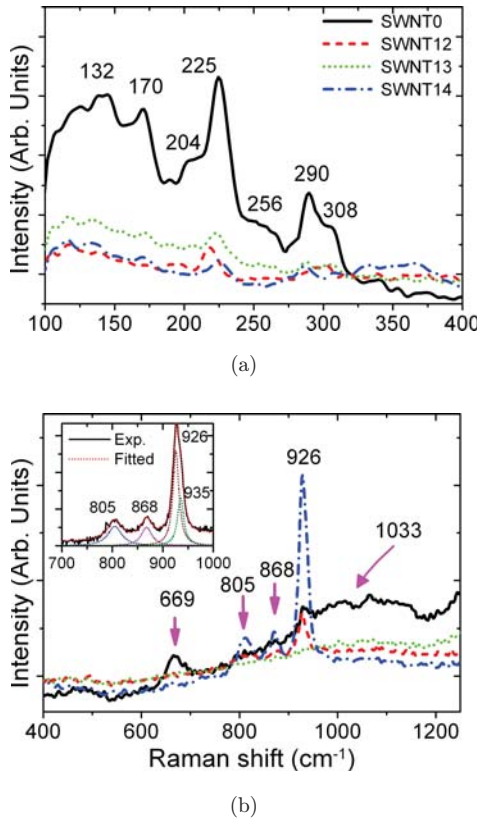


Fig. 2. Raman spectra of SWNTs (a) modification of RBM modes and (b) changes in the IFM modes.

and simultaneously decrease of intensity of D-band, indicating structural reconstruction and improvement upon ion-irradiation shown in Fig. 3(a). This is an important finding in this study. Irradiation leads to the blueshift of G' mode, whereas FWHM and intensity of this peak scale with the structural defects as shown in Fig. 3(b). FWHM and intensity increase upon 10^{12} and 10^{14} doses, whereas with the dose of 10^{13} ions/cm² it decreases.

3.3. XPS studies

Deconvoluted C_{1s} core spectra (not shown) of SWCNT before irradiation show three peaks at 284.21, 284.89, and 286.12 eV originating due to sp² carbon, sp³ carbon, and structural defects, respectively. Usually the peak of tetrahedral bonded sp³ carbon is observed near 285.5 eV¹¹ as observed for all irradiated samples, but in case of virgin SWNTs it is shifted by 0.61 eV. Amount of the sp² and sp³ hybridized carbon from the percentage of peak areas shows increase in sp² carbon and decrease in sp³ carbon after 10^{13} ions/cm² irradiation, giving clear evidence of structural improvement with a dose of

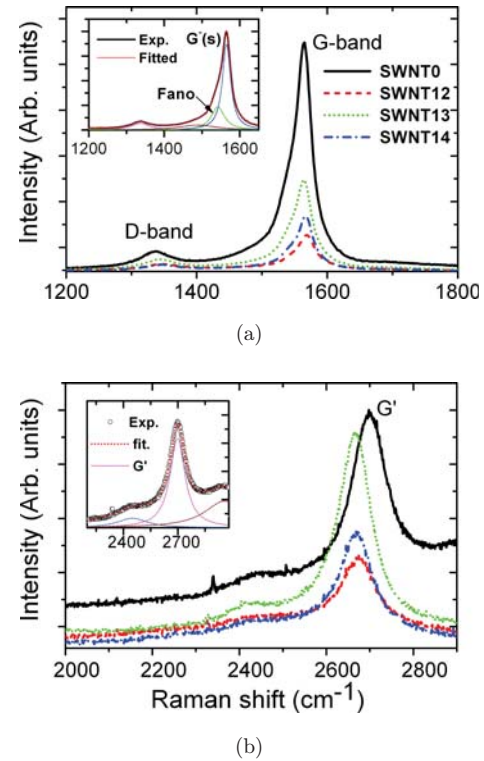


Fig. 3. Raman spectra of SWNTs (a) Characteristic D- and G-band (b) Changes in the second-order G' overtone modes.

10^{13} ions/cm². XPS survey scan spectra do not show any peak in the nitrogen core region 392–410 eV, which indicates absence of N-doping as a result of irradiation.¹² This further supports the fact that defects are created by N irradiation and the IFM Raman modes arise from phonon density of states appearing due to structural defects.

4. Conclusions

Our experiment shows that a N⁺ ion dose of 10^{13} ions/cm² can be used to heal the naturally occurring defects in the SWNTs. Raman modes at 804, 868, 926, and 935 cm⁻¹ known as IFM modes originate due to structural defects in CNTs. Ion irradiation in case of SWNTs leads to formation of vacancies and Stone–Wales defects, whereas in case of MWNTs it leads to formation of curved graphitic structure. These curved carbon structures get converted to fullerenes with higher doses.

Acknowledgments

The authors are thankful to B. K. Panigrahi and K. G. M. Nair, IGCAR, Kalpakkam for their help in

ion irradiation experiment. D. K. Singh thanks CSIR, India for the senior research fellowship.

References

1. L. Valentini, F. Mercuri, J. M. Kenny *et al.*, *Chem. Phys. Lett.* **387**, 356 (2004).
2. M. Passacantando, F. Bussolotti, A. Raulo *et al.*, *Appl. Phys. Lett.* **93**, 051911 (2008).
3. U. Ritter, H. Bernas *et al.*, *Chem. Phys. Lett.* **447**, 252 (2007).
4. U. Ritter, P. Scharff, H. Bernas *et al.*, *Carbon* **44**, 2694 (2006).
5. A. C. Dillon *et al.*, *Chem. Phys. Lett.* **401**, 522 (2005).
6. A. V. Krasheninnikov and K. Nordlund, *Nucl. Inst. Meth. B* **216**, 355 (2004).
7. A. V. Krasheninnikov and F. Banhart, *Nat. Mat.* **6**, 723 (2007).
8. R. Saito *et al.*, *Phys. Rev. B* **57**, 4145 (1998).
9. M. Kalbac, L. Kavan, M. Zúkalová and L. Dunsch, *Chem. Eur. J.* **12**, 4451 (2006).
10. V. Skákalová, J. Maultzsch, Z. Osváth, L. P. Biró and S. Roth, *Phys. Stat. Sol. (RRL)* **1**, 138 (2007).
11. S. Talapatra, P. M. Ajayan *et al.*, *Phys. Rev. Lett.* **95**, 097201 (2005).
12. F. Xu, M. Minniti, L. Papagno *et al.*, *Surf. Sci.* **601**, 2819 (2007).